

Spin structure of the doped quasi-one-dimensional copper oxide $\text{Ca}_2\text{Y}_2\text{Cu}_5\text{O}_{10}$

H. F. Fong

Department of Physics, Princeton University, Princeton, New Jersey 08544

B. Keimer

*Department of Physics, Princeton University, Princeton, New Jersey 08544
and Max-Planck-Institut für Festkörperforschung, D-70569 Stuttgart, Germany*

J. W. Lynn

Reactor Division, National Institute of Standards and Technology, Gaithersburg, Maryland 20899

A. Hayashi and R. J. Cava

Department of Chemistry, Princeton University, Princeton, New Jersey 08544

(Received 21 September 1998)

The $x=0$ parent compound of the $\text{Ca}_{2+x}\text{Y}_{2-x}\text{Cu}_5\text{O}_{10}$ family of quasi-one-dimensional copper oxides was investigated by neutron powder diffraction. Long range antiferromagnetic order, with ferromagnetic alignment of the moments along the copper oxide chains, was observed below $T_N=29.5$ K. The low temperature ordered moment is $0.92\mu_B$, close to the free ion value. The results are compared to observations on other magnetically ordered copper oxides. [S0163-1829(99)09609-5]

I. INTRODUCTION

Electronic transport in low dimensional copper oxides has been the focus of much activity during the past decade. In particular, unusual superconducting states have been observed in layered cuprates, and more recently also in cuprates with quasi-one-dimensional structures.¹ One-dimensional systems are more amenable to analytical and numerical calculations and may well hold lessons for the two-dimensional systems as well. Unfortunately, quasi-one-dimensional cuprates that can be doped, such as $(\text{Sr}, \text{Ca})_{14}\text{Cu}_{24}\text{O}_{41}$,¹ are structurally very complicated, with several electronically active units. Structurally simple quasi-one-dimensional copper oxides such as CuGeO_3 ,² SrCuO_2 , and Sr_2CuO_3 (Ref. 3) have also been widely studied, but attempts to introduce mobile charge carriers into the copper oxide chains have thus far been unsuccessful.

Recently, Hayashi *et al.*⁴ reported the synthesis of the series $\text{Ca}_{2+x}\text{Y}_{2-x}\text{Cu}_5\text{O}_{10}$ whose crystal structure consists exclusively of CuO_2 chains and Ca/Y chains that act as charge reservoirs (Fig. 1). The CuO_2 chains are formed by CuO_4 squares aligned in an edge-sharing fashion. For $x=0$, copper is in the Cu^{2+} valence state, and each copper ion carries a local spin $S=1/2$. With increasing x , the copper valence increases up to $\text{Cu}^{2.4+}$ for $x=2$, and the electrical conductivity is enhanced by several orders of magnitude. However, its temperature dependence remains insulating for all x . Susceptibility measurements indicate antiferromagnetic long range order at low temperatures for $x<1.5$, and a magnetically short range ordered state for $x>1.5$.

In this article, neutron powder diffraction is used to establish the low temperature magnetic structure of the antiferromagnetic parent compound ($x=0$). Within the CuO_2 chains, the moments are ferromagnetically aligned, and the moment size is surprisingly large (close to the free ion value). This provides a starting point for further investigations of the

magnetic structure and dynamics for $0<x<2$. The experimental procedure and results are described in Secs. II and III, and the results are discussed in Sec. IV in the context of analogous observations in other quasi-one-dimensional copper oxides.

II. EXPERIMENTAL DETAILS

A polycrystalline sample of $\text{Ca}_2\text{Y}_2\text{Cu}_5\text{O}_{10}$ was synthesized by heating a mixture of high-purity Y_2O_3 , CaCO_3 , and CuO in air at 900°C for 12 h in an Al_2O_3 crucible. The product was ground, pelletized, and heated in air at 1000°C for 120 h with several intermediate grindings, and subsequently annealed at 1000°C under an oxygen pressure of 215 ± 5 bars for another 48 h. The pellet was reground and the heat treatment repeated to ensure complete reaction.

A 5 g powder sample in a standard aluminum can was loaded into a pumped helium cryostat. The neutron diffraction measurements were carried out on the BT-1 high-resolution powder diffractometer and the BT-2 triple axis spectrometer at the research reactor at the National Institute of Standards and Technology (NIST). On BT-1, a $\text{Cu}(311)$ monochromator selected a neutron wavelength of 1.540 \AA , and a $15'$ in-pile collimator was used to collimate the beam. On BT-2, a neutron wavelength of 2.359 \AA was selected by a pyrolytic graphite (002) monochromator. A low resolution configuration with collimations $60' -40' -40'$ (before monochromator, between monochromator and sample, and between sample and detector) and a high resolution configuration with collimation $20' -20' -20'$ were used. The former configuration maximizes the count rate of the magnetic reflections, the latter was necessary to separate some reflections from nearby nuclear Bragg reflections. A pyrolytic graphite filter was placed before the sample in order to eliminate higher order contamination of the incident beam.

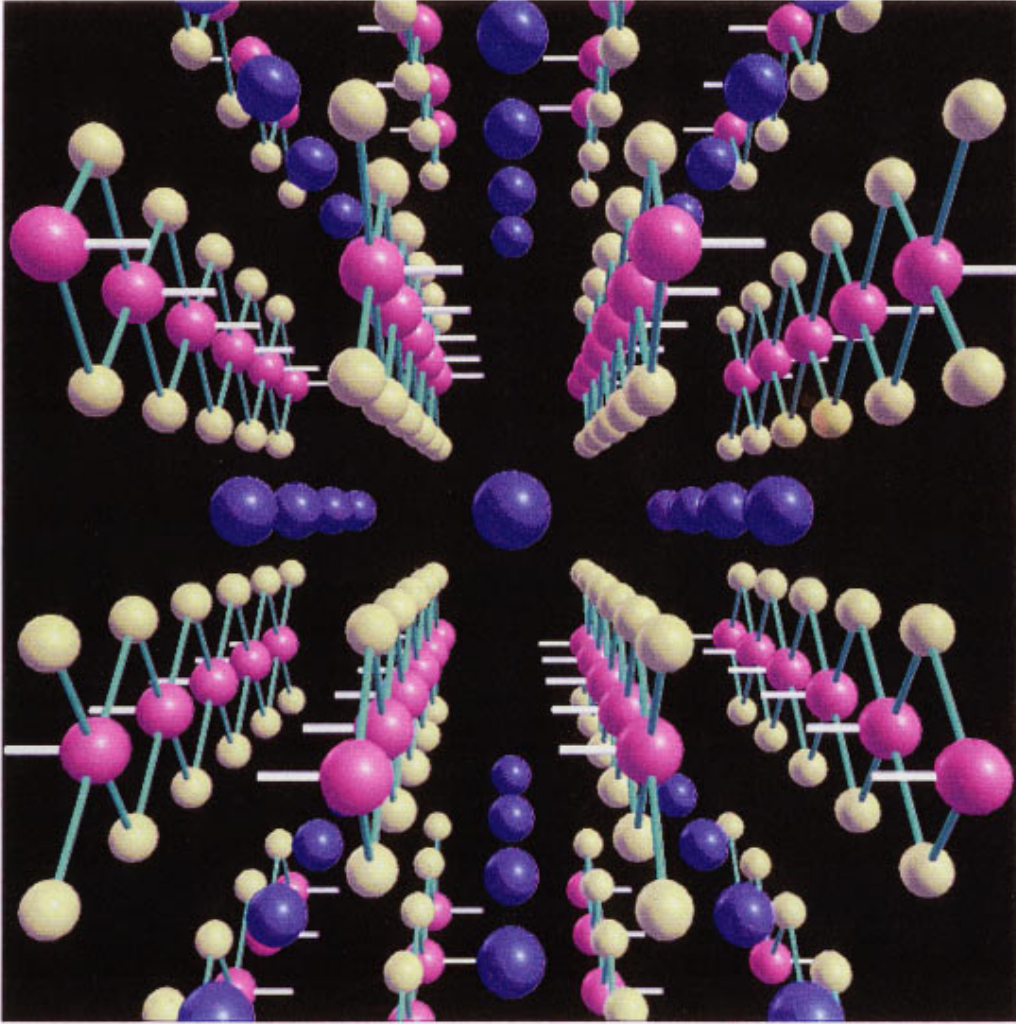


FIG. 1. (Color) View of the lattice and spin structures of $\text{Ca}_2\text{Y}_2\text{Cu}_5\text{O}_{10}$ along the \hat{a} (spin chain) direction. The \hat{b} axis runs horizontally, the \hat{c} axis vertically. Purple atoms are copper, yellow atoms are oxygen, and blue atoms are Ca or Y. The white lines indicate the spin directions. The green lines along the nearest-neighbor copper-oxygen bonds accentuate the CuO_2 chains.

III. RESULTS

As the fundamental periodicities along the CuO_2 and Ca/Y chains are different (with 4 Ca/Y atoms per 5 Cu atoms along the chains), a full description of the crystal structure of $\text{Ca}_2\text{Y}_2\text{Cu}_5\text{O}_{10}$ requires a large, monoclinic unit cell.⁵ However, as the magnetic moments reside on a sublattice that consists exclusively of the CuO_2 chains, we simplify the following discussion by employing a reduced orthorhombic unit cell containing 4 copper atoms, with lattice parameters $a = 2.818 \text{ \AA}$, $b = 6.184 \text{ \AA}$, and $c = 10.596 \text{ \AA}$ at room temperature ($a = 2.811 \text{ \AA}$, $b = 6.172 \text{ \AA}$, and $c = 10.572 \text{ \AA}$ at $T = 1.5 \text{ K}$). The CuO_2 chains run along the \hat{a} direction and are staggered along \hat{b} and \hat{c} .

Full diffraction patterns were recorded on BT-1 at temperatures 1.5, 15, 40, 100, and 300 K. While no changes were observed between 300 and 40 K, additional magnetic Bragg reflections appear at lower temperatures. In order to obtain accurate intensities of the magnetic reflections identified in this survey, additional data were taken on BT-2. The temperature dependence of the integrated intensity of the

lowest-index reflection with wave vector $\mathbf{q}_0 = \mathbf{c}^*$, measured on BT-2, is given in Fig. 2. It indicates that the Néel temperature is $T_N = (29.5 \pm 1) \text{ K}$.

The intensities of the remaining magnetic reflections were determined by subtracting the intensity at 30 K ($> T_N$) from the intensity at 1.5 K and fitting the resulting profiles to Gaussians of width equal to the instrumental resolution. A synopsis of the data and the fitted curves is given in Fig. 3. All observed magnetic reflections, listed in Table I, are of the forms $(h, k, l) = (\text{even}, \text{even}, \text{odd})$ or $(\text{odd}, \text{odd}, \text{even})$, indicating that ferromagnetic sheets lie along the $\hat{a} - \hat{b}$ plane and adjacent sheets have opposite spin directions.

In order to extract the moment size and direction from the data, the magnetic Bragg intensities have to be compared to model calculations. The elastic magnetic cross section is given by

$$\frac{d\sigma}{d\Omega} \sim f^2(\mathbf{q}) \frac{\mu^2}{\mu_B^2} \delta(\mathbf{q} - \mathbf{q}_0) \times \exp(-2W(\mathbf{q})) |F_M(\mathbf{q})|^2 (1 - \hat{q} \cdot \hat{\eta})^2, \quad (1)$$

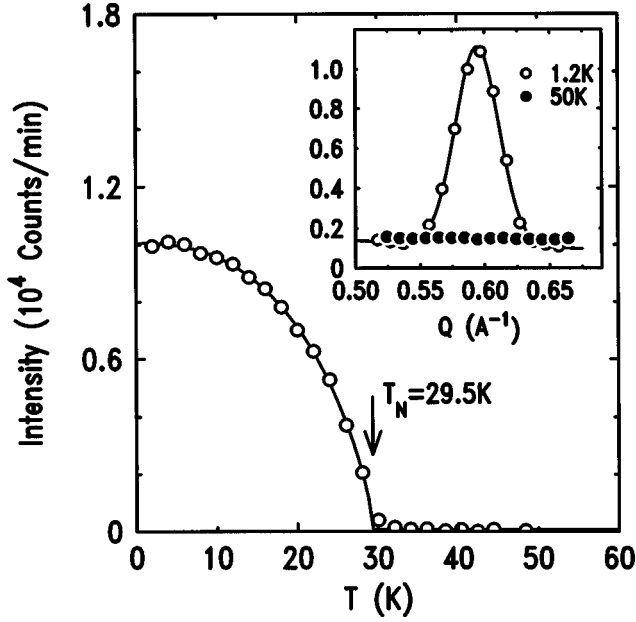


FIG. 2. Integrated intensity of the (001) magnetic Bragg reflection. The line is a guide to the eye. The inset shows typical data obtained above and below the Néel temperature $T_N = 29.5$ K.

where $f(\mathbf{q})$ is the magnetic form factor, μ the magnitude of the ordered moment, \mathbf{q}_0 a magnetic reciprocal lattice vector, $\exp(-2W(\mathbf{q}))$ the Debye-Waller factor (taken to be 1 for the low temperatures investigated here), $|F_M(\mathbf{q}=\mathbf{q}_0)|^2 = 16$ the magnetic structure factor, and $\hat{\eta}$ is the spin direction. Clearly, observation of the (001) reflection precludes $\hat{\eta} \parallel \hat{c}$. We have considered two simple alternatives, with $\hat{\eta}$ along \hat{a} or \hat{b} , respectively. In order to distinguish these two possibilities, a model of the anisotropic form factor $f(\mathbf{q})$ is needed. We assume that the unpaired electron is predominantly of Cu $3d_{x^2-y^2}$ character; limitations of this assumption are discussed below. The Cu $d_{x^2-y^2}$ orbital is approximated by

$$\psi(\mathbf{r}) = A \left(\frac{r}{a_0} \right)^2 e^{-r/3a_0} \sin^2 \theta \cos 2\phi, \quad (2)$$

where A is the normalization constant, and a_0 is an adjustable parameter. The corresponding form factor is $f(\mathbf{q})$

$= \int |\psi(\mathbf{r})|^2 e^{i\mathbf{q} \cdot \mathbf{r}} d^3r$. After a partial wave expansion, the angular part of the Fourier transform can be carried out analytically, so that

$$\begin{aligned} f(\mathbf{q}) = & \langle j_0(q) \rangle + \frac{5}{7} (3 \cos^2 \theta_q - 1) \langle j_2(q) \rangle \\ & + \left(\frac{15}{8} \cos 4\phi_q \sin^4 \theta_q + \frac{3}{56} (3 - 30 \cos^2 \theta_q \right. \\ & \left. + 35 \cos^4 \theta_q) \right) \langle j_4(q) \rangle, \end{aligned} \quad (3)$$

where $\langle j_l(q) \rangle = \int r^2 dr A^2 (r/a_0^7) \exp(-2r/3a_0) j_l(qr)$. The factor a_0 was adjusted to get good agreement with an extensive set of magnetic reflections measured in crystals of antiferromagnetic $\text{YBa}_2\text{Cu}_3\text{O}_6$,⁶ whose sublattice magnetization also arises from Cu $d_{x^2-y^2}$ electrons.

The calculated form factor is given in Table I, as are the calculated peak intensities (corrected for the form factor, the phase space factor $1/\sin \theta \sin 2\theta$, and the peak multiplicities) for both $\hat{\eta} \parallel \hat{a}$ and $\hat{\eta} \parallel \hat{b}$. While the (021) peak intensity predicted in the former model is much larger than observed, a good fit of all observed intensities is obtained for $\hat{\eta} \parallel \hat{b}$. In order to eliminate uncertainties associated with the superlattice modulation along the \hat{a} direction,⁵ we only used nuclear reflections of the form $(0, k, l)$ to extract μ . The result is $\mu = 0.92 \pm 0.08 \mu_B$, close to the value $\mu = 1 \mu_B$ of the free Cu^{2+} ion. A pictorial representation of the spin structure below T_N is given in Fig. 1.

IV. DISCUSSION

At first sight, the ferromagnetic alignment of the spins along the chains appears consistent with the Goodenough-Kanamori-Anderson rules⁷ that predict ferromagnetic interactions for superexchange involving intermediate states in two orthogonal orbitals. As the Cu-O-Cu bond angle is 93° in $\text{Ca}_2\text{Y}_2\text{Cu}_5\text{O}_{10}$, this condition appears to be satisfied for the two oxygen p -orbitals connecting nearest-neighbor copper moments. Edge-sharing copper oxide chains in other compounds such as $\text{La}_5\text{Ca}_9\text{Cu}_{24}\text{O}_{41}$,⁸ $\text{La}_6\text{Ca}_8\text{Cu}_{24}\text{O}_{41}$,⁹ and Li_2CuO_2 (Ref. 10) also order ferromagnetically. However, both the large ordered moment and the positive Curie-Weiss

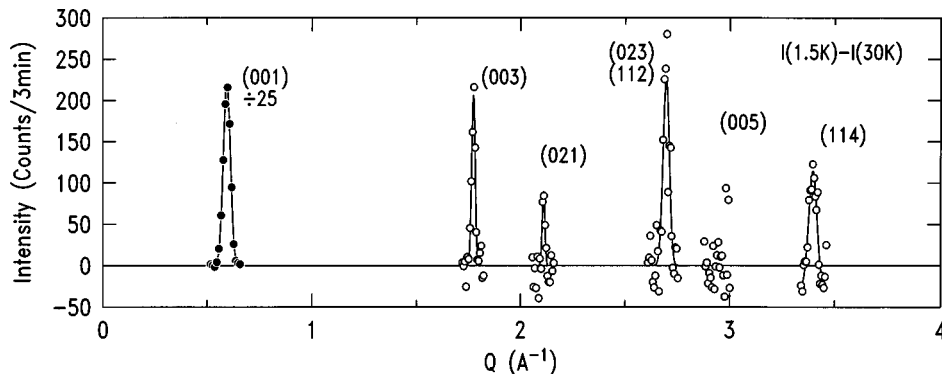


FIG. 3. Magnetic diffraction pattern obtained by subtracting the intensity at $T = 30$ K ($> T_N$) from the intensity at 1.5 K ($< T_N$). The filled (open) circles represent data taken with coarse (fine) momentum resolution. The lines are the results of fits to resolution-limited Gaussians.

TABLE I. Integrated intensities of observed magnetic Bragg reflections. The modeled intensities are scaled so that the (001) intensities match. The form factors were calculated as discussed in the text.

(h,k,l)	$ q (\text{\AA}^{-1})$	$ f(\mathbf{q}) ^2$	Data	$\hat{\eta}\parallel\hat{a}$	$\hat{\eta}\parallel\hat{b}$
(001)	0.5943	0.96	347 ± 11	347	347
(003)	1.7829	0.67	15.6 ± 1.6	28.44	28.44
(021)	2.12	0.81	6.1 ± 1.4	50.22	3.96
(023)/(112)	2.706/2.728	0.57/0.43	30.7 ± 10	23.04/11.16	10.08/29.52
(005)	2.972	0.30	0 ± 13	5.22	5.22
(114)	3.4	0.26	25.0 ± 3.8	8.28	13.32

temperature extracted from the high temperature uniform susceptibility of $\text{Ca}_2\text{Y}_2\text{Cu}_5\text{O}_{10}$ (Ref. 4) are inconsistent with predominantly one-dimensional, ferromagnetic spin-spin interactions.

Indeed, recent experimental and theoretical research on copper oxides with quasi-one-dimensional structures has revealed a more complex picture. First, the observation that the spin-Peierls compound CuGeO_3 has antiferromagnetic nearest-neighbor interactions² despite the 99° Cu-O-Cu bond angle has prompted a more careful investigation of the superexchange rules for edge-sharing copper oxide chains.¹² It was found that the magnitude and sign of the nearest-neighbor exchange coupling are sensitive functions of side groups that hybridize with the oxygen p -orbital; in general, these hybridized orbitals are no longer orthogonal.

Second, a recent inelastic neutron scattering study of Li_2CuO_2 , whose CuO_2 chains are arranged in a fashion similar to $\text{Ca}_2\text{Y}_2\text{Cu}_5\text{O}_{10}$, has revealed a rather complex, three-dimensional set of magnetic interactions with competing nearest and next nearest neighbor couplings along the chains.¹¹ The nearest neighbor interaction is actually antiferromagnetic, as in CuGeO_3 . Despite the different interchain distances and the different nature of the side groups, the ordering pattern as well as the size and direction of the ordered moment in the antiferromagnetically ordered phase of $\text{Ca}_2\text{Y}_2\text{Cu}_5\text{O}_{10}$ is identical to that of Li_2CuO_2 .¹⁰ This is surprising in view of the theoretical work of Ref. 12 and merits further consideration. It also suggests that some of the theo-

retical analysis performed on Li_2CuO_2 , where single crystals are available and our microscopic understanding is more advanced, carries over to $\text{Ca}_2\text{Y}_2\text{Cu}_5\text{O}_{10}$. In particular, the large moment size of Li_2CuO_2 was attributed to a combination of the three-dimensional nature of the interactions and a large exchange anisotropy (which results in a large spin wave gap).¹¹ Band structure calculations indicate that a significant fraction of the moment actually resides on the bridging oxygen ions.¹³ (If this is the case for $\text{Ca}_2\text{Y}_2\text{Cu}_5\text{O}_{10}$, the form factor calculation above will have to be modified.) Competing antiferromagnetic interactions would also provide an explanation of the positive Curie-Weiss temperature measured in $\text{Ca}_2\text{Y}_2\text{Cu}_5\text{O}_{10}$.

In conclusion, $\text{Ca}_2\text{Y}_2\text{Cu}_5\text{O}_{10}$ joins a growing number of copper oxides with intriguing magnetic properties. In this compound, the Ca/Y ratio is an additional degree of freedom that results in the introduction of holes on the spin chains. The results reported here provide a good starting point for further investigations of the short range ordered state observed at high hole concentrations.

ACKNOWLEDGMENTS

We thank L. Kleinwaks for his contributions at the early stages of this work, and Q. Huang for useful discussions. The work was supported by the National Science Foundation under Grant No. DMR-9400362, and by the Packard and Sloan Foundations.

¹M. Uehara, T. Nagata, J. Akimitsu, H. Takahashi, N. Mori, and K. Kinoshita, *J. Phys. Soc. Jpn.* **65**, 2764 (1996).

²M. Hase, I. Terasaki, and K. Uchinokura, *Phys. Rev. Lett.* **70**, 3651 (1993).

³N. Motoyama, H. Eisaki, and S. Uchida, *Phys. Rev. Lett.* **76**, 3212 (1996).

⁴A. Hayashi, B. Batlogg, and R. J. Cava, *Phys. Rev. B* **58**, 2678 (1998).

⁵P. K. Davies, *J. Solid State Chem.* **95**, 365 (1991).

⁶S. Shamoto, M. Sato, J. M. Tranquada, B. J. Sternlieb, and G. Shirane, *Phys. Rev. B* **48**, 13 817 (1993) and references therein.

⁷J. B. Goodenough, *Magnetism and the Chemical Bond* (Wiley, New York, 1963); P. W. Anderson, *Solid State Phys.* **14**, 99 (1963).

⁸M. Matsuda, K. M. Kojima, Y. J. Uemura, J. L. Zarestky, K. Nakajima, K. Kakurai, T. Yokoo, S. M. Shapiro, and G. Shirane, *Phys. Rev. B* **57**, 11 467 (1998).

⁹M. Matsuda, K. Katsumata, T. Yokoo, S. M. Shapiro, and G. Shirane, *Phys. Rev. B* **54**, R15 626 (1996).

¹⁰F. Sapina, J. Rodriguez-Carvajal, M. J. Sanchis, R. Ibanez, A. Beltran, and D. Beltran, *Solid State Commun.* **74**, 779 (1990).

¹¹M. Boehm, S. Coad, B. Roessli, A. Zheludev, M. Zolliker, P. Böni, D. M. Paul, H. Eisaki, N. Motoyama, and S. Uchida, *Europhys. Lett.* **43**, 77 (1998).

¹²W. Geertsma and D. Khomskii, *Phys. Rev. B* **54**, 3011 (1996).

¹³R. Weht and W. E. Pickett, *Phys. Rev. Lett.* **81**, 2502 (1998).